



Cite this: *Sustainable Food Technol.*, 2024, 2, 400

## Development of carboxymethyl cellulose–chitosan based antibacterial films incorporating a *Persicaria minor* Huds. essential oil nanoemulsion

Yu-Hsuan How,<sup>a</sup> Emily Min-Yan Lim,<sup>a</sup> Ianne Kong,<sup>a</sup> Phei-Er Kee <sup>b</sup> and Liew-Phing Pui<sup>\*a</sup>

As plastic waste has continued to increase over the years, there is an appeal for environmental-friendly packaging containing bioactive components such as essential oil for food packaging. However, the loss of activity and insolubility of essential oil in biopolymer-based packaging film remains a challenge. Hence, this study aimed to develop a carboxymethyl cellulose (CMC)–chitosan (CS) based antibacterial film containing a *Persicaria minor* Huds. essential oil nanoemulsion. The coarse-emulsified and nanoemulsified *P. minor* Huds. essential oils were evaluated to select the desirable emulsion type for the polymer-based film. Different concentrations of the selected essential oil emulsion (0, 4%, 8%, and 12% v/v) were incorporated into the 1.5 : 1% (w/v) CMC–CS based film. The nanoemulsion exhibited a smaller droplet size, lower whiteness index, and higher antibacterial activity as compared to the coarse emulsion. The addition of the *P. minor* Huds. essential oil nanoemulsion in the composite film lowered Young's modulus, resulting in a more flexible and less rigid film. The 12% (v/v) essential oil nanoemulsion film displayed desirable characteristics with 0.15 mm thickness, 11.52  $A_{600}/\text{mm}$  opacity, 65.5% water solubility, and the lowest moisture content (19.21%) among the different concentrations. Additionally, the 12% (v/v) nanoemulsion CMC–CS based film had the least irregular surface structure, highest antioxidant activity (4.25 mg TE g<sup>-1</sup>), and antibacterial activity against *Escherichia coli* and *Bacillus subtilis* (7.19 and 7.85 mm) as compared to other concentrations. The present work demonstrates the potential of the *P. minor* Huds. essential oil nanoemulsion in CMC–CS based film as bioactive packaging to prevent the presence of common foodborne pathogens in food products.

Received 4th October 2023  
Accepted 17th December 2023

DOI: 10.1039/d3fb00183k  
[rsc.li/susfoodtech](http://rsc.li/susfoodtech)

### Sustainability spotlight

Every year, approximately 150 million tonnes of plastic is manufactured globally. The plastic production and consumption have continuously increased and this has led to severe environmental contamination. The edible film produced in this study is one of the alternatives to reduce the usage of plastic films in the food industry. The edible film is made up of food-grade biodegradable polymers which offer advantages such as renewability, waste reduction, and the ability to be consumed as an integral part of the food product. This work is aligned with the sustainable development goals (SDG) 12, specifically goal target 12.5 which states 'By 2030, substantially reduce waste generation through prevention, reduction, recycling and reuse' by presenting a promising alternative to synthetic plastic film as food packaging.

## Introduction

The increasing global awareness of environmental protection and food safety has sparked considerable interest in the development of novel packaging systems based on biodegradable polymers. These systems often utilize natural food-grade polymers, such as polysaccharides, proteins, and lipids, as alternatives to synthetic packaging systems.<sup>1</sup> Biodegradable film

packaging offers important advantages, including renewability, waste reduction, and the ability to be consumed as an integral part of the food product.<sup>2</sup> Additionally, it aims to preserve food quality and extend shelf life by minimizing the exchange of moisture, lipids, volatiles, and gases, while also acting as an effective carrier for bioactive compounds such as food additives, antioxidants, and antimicrobial compounds.<sup>3</sup> Materials such as chitosan (CS) and other polysaccharide-based films have proven to be an effective barrier against nonpolar aromatic compounds, thereby preventing aroma loss and oxidation.<sup>4</sup> On the other hand, hydrocolloid-based films, such as carboxymethyl cellulose (CMC), can retain moisture and reduce fat uptake in deep-fat fried food.<sup>5</sup>

<sup>a</sup>Department of Food Science and Nutrition, Faculty of Applied Sciences, UCSI University, Cheras, Wilayah Persekutuan Kuala Lumpur, Malaysia. E-mail: [zoepui123@gmail.com](mailto:zoepui123@gmail.com)

<sup>b</sup>Biorefinery and Bioprocessing Engineering Laboratory, Department of Chemical Engineering and Materials Science, Yuan Ze University, Chungli, Taoyuan 320, Taiwan



CS, a chitin derivative synthesized by living organisms, can be obtained from renewable sources such as seafood industry waste.<sup>4</sup> It is a promising film component owing to its exceptional film-forming properties, selective permeability to gases, non-toxicity, and antimicrobial properties.<sup>6</sup> CMC, a cellulose derivative, is an ideal biopolymer to develop clear film with excellent gas and lipid barrier properties.<sup>7</sup> CMC has been widely applied as a film-forming biopolymer owing to its non-toxicity, cost-effectiveness, high solubility in water, ability to induce viscosity in solution, and good film-forming capabilities.<sup>8</sup> However, the use of polysaccharide-based films is limited due to their hydrophilic nature, which makes them susceptible to moisture and can negatively impact their mechanical properties.<sup>9,10</sup> To overcome these challenges, the development of CS and CMC biopolymer composites is suggested, combining the unique properties of both biopolymers. This is supported by several studies demonstrating improved barrier properties against moisture and increased tensile strength.<sup>9,11,12</sup>

Microbial contamination in food is a serious issue globally. While synthetic preservatives are commonly used to control microbial growth in food products, their potential adverse side effects have raised concerns about the safety of food products containing these synthetic chemicals. To address this issue, natural antimicrobial compounds, such as essential oils, are explored as promising alternatives. *Persicaria minor* Huds., also known as kesum in Malay, is recognized for its medicinal properties, and its essential oil is used in the food, pharmaceutical, and perfumery industries. It is an aromatic plant that produces high levels of essential oil (72.54%) containing aliphatic aldehydes.<sup>13</sup> *Persicaria minor* Huds. essential oil is categorized as Generally Recognized as Safe (GRAS) and reported to exhibit antibacterial properties against numerous food spoilage and pathogenic microorganisms such as *Salmonella enterica*, *Staphylococcus aureus*, *Streptococcus pneumoniae*, *Streptococcus pyogenes*, and *Pseudomonas aeruginosa*.<sup>14</sup>

Despite their antibacterial properties, essential oils have practical limitations due to organoleptic acceptance levels at high dosage and poor physicochemical properties, such as water insolubility and high volatility, which makes it challenging to incorporate them into films.<sup>15</sup> Nanoemulsion technology is a promising strategy to overcome the poor physicochemical properties of essential oils by dispersing them in oil-in-water (O/W) emulsions, resulting in enhanced stability and compatibility with a variety of biodegradable matrices.<sup>16</sup> This approach could also enhance the functional properties of essential oils, allowing them to be a more versatile ingredient in food and beverage formulations.<sup>17,18</sup>

To the best of our knowledge, there has yet to be a study on antibacterial films using CMC and CS composites with nanoemulsified *P. minor* essential oil. The coarse-emulsified and nanoemulsified *P. minor* essential oil were first evaluated on the droplet size, zeta-potential, and antibacterial properties. Further investigation was carried out on the physicochemical properties, mechanical properties, microstructure, and antioxidant and antibacterial activity of the CMC-CS based composite film containing different concentrations of the *P. minor* essential oil nanoemulsion.

## Materials and methods

### Materials

*Persicaria minor* Huds. leaves were purchased from a local market at Malacca, Malaysia. Tween 80, oleic acid, Mueller-Hinton agar, and acetic acid were purchased from Thermo Fisher Scientific, USA. Chitosan, sodium hydroxide, glycerol, carboxymethyl cellulose, 2,4,6-tri(2-pyridyl)-1,3,5-triazine (TPTZ), acetate buffer, and ferric chloride were purchased from Chemsoln, India. The nutrient broth was purchased from Merck, Germany, while the tetracycline disc was purchased from Oxoid, UK. *Bacillus subtilis* and *Escherichia coli* were obtained from UCSI University, Malaysia.

### Extraction of *Persicaria minor* Huds. essential oil

The *Persicaria minor* Huds. essential oil was extracted through hydro-distillation using a Clevenger-type apparatus and a heating mantle according to Singh *et al.*<sup>19</sup> Cleaned *P. minor* Huds. leaves (Malacca, Malaysia) were removed from its stem. The leaves (1 kg) were placed in a flask with distilled water (2.5 L) and heated at 120 °C for 5–6 h. The yellow-coloured essential oil was collected (1 mL) using a micropipette and stored in a sealed vial at 4 °C prior to use.

### Preparation of the *Persicaria minor* Huds. essential oil coarse emulsion and nanoemulsion

The coarse emulsion was prepared by mixing distilled water with *P. minor* essential oil (5% v/v) and Tween 80 (30% wt. oil) (Thermo Fisher Scientific, USA) using a T25 digital Ultra-TURRAX high-speed homogenizer (IKA, Germany) at 9000–12 000 rpm for 5 min. On the other hand, the nanoemulsion (NE) was produced according to Noori *et al.*<sup>20</sup> with modifications, by mixing *P. minor* essential oil (5% (v/v)) and Tween 80 (30% wt. oil) in distilled water. The mixtures were homogenized using an Avestin EmulsiFlex-C3 high-pressure homogenizer (Avestin, Canada) at 12 000–15 000 psi homogenization pressure and 4–5 homogenization cycles.

### Preparation of the carboxymethyl cellulose–chitosan (CMC–CS) based film-forming solution with *Persicaria minor* Huds. essential oil emulsions

CMC–CS based films were prepared as described by Noshirvani *et al.*<sup>6</sup> with some modifications. The CS powder (1% (w/v)) (Chemsoln, India) was dispersed in acidic water (0.5% v/v acetic acid in 100 mL distilled water) and stirred overnight (500 rpm) using a magnetic stirrer. The pH of the solution was adjusted to pH 6.7 with NaOH (3 M) (Chemsoln, India). CMC powder (1.5% (w/v)) (Chemsoln, India) was dissolved in distilled water (100 mL) and stirred continuously at 60 °C for 40 min.

The two solutions were mixed using a T25 digital Ultra-TURRAX high-speed homogenizer (IKA, Germany) at 12 000 rpm, and 0.6 mL of 0.3% (v/v) Tween 80 was incorporated as an emulsifier. After 5 min, 0.9 mL of 0.45% (v/v) oleic acid (Thermo Fisher Scientific, USA) was added, resulting in a turbid and milky-white mixture. Different concentrations of



nanoemulsified essential oil (0%, 4%, 8%, and 12% (v/v)) were respectively added in the CMC-CS based film-forming solution. One millilitre of glycerol (Chemsoln, India) at 40% (v/w) was added into the mixture and homogenized for 5 min. Then 25 mL of film-forming mixtures were poured into a glass Petri dish (90 mm × 15 mm) and dried in a ventilated oven (Memmert ULM 500, Germany) at 40 °C for 48 h. The formulation and preparation steps had been optimized in an unpublished preliminary trial to ensure a uniformly dispersed composite film.

#### Average droplet size, polydispersity index, and zeta-potential of essential oil emulsions

The essential oil solution was first diluted with distilled water at a 1 : 16 ratio to avoid multiple scattering effects. The average droplet size, polydispersity index, and zeta-potential were then analysed using a Malvern ZetaSizer Nano ZS (Malvern Instruments, UK) according to Acevedo-Fani *et al.*<sup>21</sup> The droplet size of emulsions was assessed using dynamic light scattering at 633 nm with a back scatter detector at 173°, while the zeta-potential at the oil droplet interface was determined through phase-analysis light scattering.

#### Whiteness index of essential oil emulsions

The whiteness of the essential oil solution was determined using a ColorFlex EZ colorimeter (HunterLab, USA) with an illuminant, D65, and the 10° observer angle according to Acevedo-Fani *et al.*<sup>21</sup> The CIE chromaticity coordinates  $L^*$  (lightness = 0 and darkness = 100),  $a^*$  (red (+) and green (-)), and  $b^*$  (yellow (+) and blue (-)) were used to calculate the whiteness index using eqn (1):

$$\text{Whiteness index} = 100 - \sqrt{(100 - L^*)^2 + (a^{*2} + b^{*2})} \quad (1)$$

#### Antibacterial activity of essential oil emulsions and composite films with essential oil emulsions

The antibacterial activity of the essential oil solutions and composite films with essential oils was assessed using the agar well diffusion method.<sup>22</sup> One colony of *Bacillus subtilis* and *Escherichia coli* (UCSI University, Malaysia) was inoculated in 10 mL nutrient broth and incubated at 37 °C for 18–24 h, respectively. The cultures were then adjusted to a concentration of approximately 8–9 log<sub>10</sub> CFU per mL and 50 µL of the bacterial suspensions were spread on Mueller–Hinton agar. The positive control was treated with tetracycline solution, while distilled water was used as the negative control. For the essential oil solutions, agar wells were punctured (6 mm diameter) and 20 µL of essential oil solutions were pipetted into the wells. On the other hand, 6 mm of the circular composite film with 4–12% (v/v) essential oils were cut and placed on the Mueller–Hinton agar. A tetracycline disc (30 µg g<sup>-1</sup>) (Oxoid, UK) was used as positive control, while CMC-CS based films with 0% essential oil concentration served as the negative control. The agar medium plates were then incubated

at 37 °C for 24 h, and the diameter of inhibition zones (in mm) was measured.

#### Colour of composite films with essential oil emulsions

The colour of the composite films was determined using a ColorFlex EZ colorimeter (HunterLab, USA) with an illuminant, D65, and the 10° observer angle according to Acevedo-Fani *et al.*<sup>21</sup> The CIE chromaticity coordinates  $L^*$  (lightness = 0 and darkness = 100),  $a^*$  (red (+) and green (-)), and  $b^*$  (yellow (+) and blue (-)) were used to calculate the colour difference using eqn (2):

$$\Delta E = \sqrt{(L^* - L)^2 + (a^* - a)^2 + (b^* - b)^2} \quad (2)$$

$L$ ,  $a$ , and  $b$  are the colour parameter values of the standard ( $L = 72.84$ ,  $a = -1.44$ ,  $b = 4.98$ ), while  $L^*$ ,  $a^*$ , and  $b^*$  are the colour parameter values of the composite films.

#### Opacity of composite films with essential oil emulsions

Film opacity was evaluated according to Zuo *et al.*<sup>23</sup> with minor modifications. The composite films were cut into 1 cm × 3 cm pieces and placed into a plastic cuvette. The absorbance was measured at 600 nm using a spectrophotometer (UviLine 9400, Secoman, France) and an empty cuvette was used as blank. The opacity of films was calculated using eqn (3):

$$\text{Opacity} = \frac{A_{600}}{\text{Thickness (mm)}} \quad (3)$$

#### Thickness of composite films with essential oil emulsions

The thickness of the film was measured using a micrometer screw gauge. The measurements were collected at five different points of the films to obtain average values.<sup>24</sup>

#### Water solubility of composite films with essential oil emulsions

Water solubility of films was evaluated according to Gahruei *et al.*<sup>22</sup> with modifications. The 2 cm × 2 cm composite films were dried at 60 °C for 24 h and weighed. The dried films were then immersed in 50 mL of distilled water at 25 °C for 30 min under constant agitation at 200 rpm using an orbital shaker. The film residuals were filtered and dried at 60 °C for 24 h to achieve a constant weight. The final weight was determined, and the percentage of solubility was calculated using eqn (4):

$$\text{Solubility (\%)} = \frac{\text{Initial dry weight} - \text{Final dry weight}}{\text{Initial dry weight}} \times 100\% \quad (4)$$

#### Moisture content of composite films with essential oil emulsions

The moisture content of the film was measured according to Lee *et al.*<sup>25</sup> with slight modification. The weight of the 2 cm × 2 cm film was measured and it was dried for 24 h in a hot air oven at



60 °C. The final weight of the dried films was measured, and the moisture content was calculated using eqn (5):

$$\text{Moisture content (\%)} = \frac{\text{Initial dry weight} - \text{Final dry weight}}{\text{Initial dry weight}} \times 100\% \quad (5)$$

### Scanning electron microscopy of composite films with essential oil emulsions

The superficial and internal microstructure of the film surface was analysed using a scanning electron microscope (SEM) (TM30000, Hitachi, Japan). The composite films were cut into 2 cm × 2 cm pieces and mounted on an aluminium stub using double-sided copper tape and coated with a thin layer of gold. The SEM was operated at an acceleration voltage of 5 kV with 100× magnification.<sup>26</sup>

### Tensile strength, elongation at break and Young's modulus of composite films with essential oil emulsions

The mechanical properties of the film were determined using a tensile strength machine (LF-Plus, LLOYD Instruments, UK).<sup>27</sup> The composite film strip (60 mm × 15 mm) was conditioned in a desiccator containing saturated silica gel at 25 °C for 48 h. The pre-conditioned film was subjected to a tensile test performed at a cross-head speed of 20 mm min<sup>-1</sup>, an initial grip separation of 40 mm, and using a load cell of 5 kg. The peak load (N) and peak extension (mm) readings were directly obtained from the machine. Tensile strength, elongation at break, and Young's modulus were calculated according to eqn (6)–(8), respectively.

$$\text{Tensile strength (mPa)} = \frac{\text{Peak load (N)}}{\text{Cross-sectional area (mm}^2\text{)}} \quad (6)$$

$$\text{Elongation at break (\%)} = \frac{\text{Final length of ruptured film (mm)}}{\text{Initial grip length (mm)}} \quad (7)$$

$$\text{Young's modulus (mPa)} = \frac{\text{Tensile strength (MPa)}}{\text{Elongation at break (\%)}} \quad (8)$$

### Ferric reducing antioxidant power (FRAP) assay of composite films with essential oil emulsions

A 0.025 g composite film was extracted in 2 mL of 75% methanol (Chemsoln, Malaysia) for 30 min in an ultrasound water bath at 25 °C. The FRAP reagent was prepared by mixing 25 mL of 300 mmol L<sup>-1</sup> acetate buffer (Chemsoln, Malaysia), 2.5 mL of 10 mmol L<sup>-1</sup> 2,4,6-tri(2-pyridyl)-1,3,5-triazine (TPTZ) (Chemsoln, Malaysia) stock solution, and 2.5 mL of 20 mmol L<sup>-1</sup> ferric chloride solution (Chemsoln, Malaysia) in a 10 : 1 : 1 ratio. The composite film was mixed with 2.7 mL of FRAP reagent, vortexed, and incubated at 37 °C for 10 min. The absorbance was measured at 593 nm using a spectrophotometer. The blank was prepared using 300 μL of methanol with 2.7 mL of FRAP

reagent. Trolox was used as a standard and the FRAP assay was expressed as mg Trolox equivalent per g film.<sup>28</sup>

### Statistical analysis

The statistical significance of the experimental data was analysed using the SPSS software (Version 25, SPSS Inc., Chicago IL, USA) with a significance level of  $p < 0.05$ . All the analyses were conducted in triplicate. The independent *T*-test was used to analyse the data between coarse-emulsified and nanoemulsified essential oil, while one-way analysis of variance (ANOVA) and Tukey's post hoc test were employed to analyse data between composite films with different concentrations of nanoemulsified essential oil.

## Results and discussion

### Average droplet size, polydispersity index, zeta-potential and whiteness index of essential oil emulsions

The droplet size and distribution are considered essential parameters to ensure emulsion stability. As demonstrated in Fig. 1, the particle size distribution of the coarse-emulsified *P. minor* Huds. essential oil from this study was multimodal, presenting several peaks corresponding to oil droplets of different sizes, whereas the particle size distribution of nanoemulsified essential oil was monomodal with a narrow distribution.<sup>29</sup> It was observed that nanoemulsified essential oil presented the highest intensity peak at the 91 nm region indicating that most of the droplets had small diameters after high-pressure homogenization. On the other hand, coarse-emulsified essential oil had larger droplet diameter at the average of 245 nm. The residual intensity peak of the coarse emulsion that is close to the detection limit of the equipment (5600 nm) suggested that the larger oil droplets were not disrupted.

The particle size of the essential oil nanoemulsion was smaller by 62.5% as compared to the coarse emulsion (Table 1). The smaller size displayed by nanoemulsified essential oil is favourable as smaller particle sizes enhance kinetic stability, solubility, and functionality as a carrier of *P. minor* Huds. essential oil.<sup>30</sup> Other studies had reported larger particle size ranging from 170 to 500 nm for nanoemulsions as compared to this study (91 nm). This could be attributed to the different process and active ingredients used by other studies where lipids, surfactants, and functional compounds were incorporated into the biopolymer matrix solution prior to the homogenisation process to prepare the coating solution in one step.<sup>21,31</sup>

The polydispersity index (PDI) value measures the heterogeneity in the droplet size distribution. PDI values close to 0 indicate homogeneous size distributions, whereas PDI values close to 1 indicate heterogeneous size distributions. Higher values also indicate greater variability in particle size and poor stability.<sup>32</sup> As shown in Table 1, the PDI values of the *P. minor* Huds. essential oil coarse emulsion are 61% lower than those of the nanoemulsion. The PDI value obtained for the essential oil nanoemulsion (PDI < 0.3) exhibited a narrow pattern of size distribution and uniformity of the emulsion droplets which was



## Size Distribution by Intensity

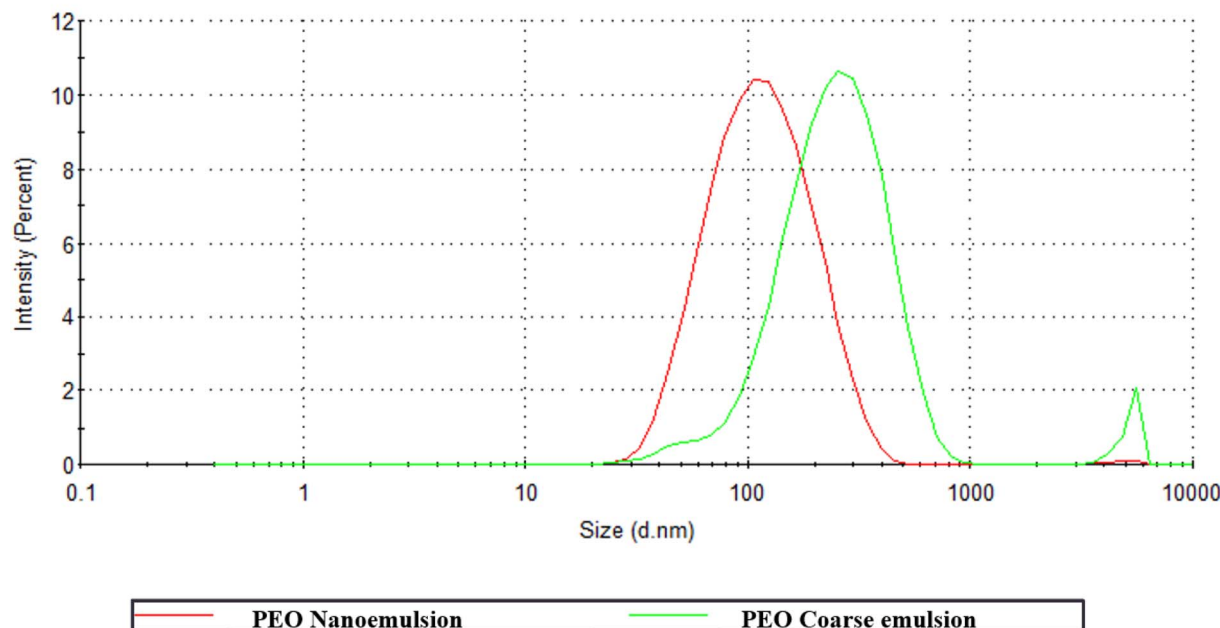


Fig. 1 Particle size distribution graph of the *Persicaria minor* Huds. essential oil coarse emulsion (green) and nanoemulsion (red).

Table 1 Average droplet size, polydispersity index, zeta-potential, and whiteness index of coarse-emulsified and nanoemulsified *Persicaria minor* Huds. essential oil solutions<sup>a</sup>

Emulsion types	<i>Persicaria minor</i> Huds. essential oil solution	
	Coarse emulsion	Nanoemulsion
Average droplet size (nm)	243.00 ± 0.60 <sup>A</sup>	91.00 ± 0.20 <sup>B</sup>
Polydispersity index	0.414 ± 0.010 <sup>A</sup>	0.163 ± 0.000 <sup>B</sup>
Zeta-potential (mV)	-27.00 ± 0.20 <sup>B</sup>	-26.00 ± 0.50 <sup>A</sup>
Whiteness index	87.37 ± 0.00 <sup>A</sup>	78.14 ± 0.01 <sup>B</sup>

<sup>a</sup> The results are expressed as mean ± standard deviation ( $n = 3$ ). <sup>AB</sup> means that in the same row there is significant difference ( $p < 0.05$ ) via an independent *t*-test.

suitable for film formulation. It is known that nanoemulsions are kinetically stable due to their small sizes, however they can be thermodynamically unstable, and thus lack in long-term stability.<sup>33</sup> In order to overcome this challenge, the nanoemulsion could be immobilized in a biopolymer matrix, thus enhancing the stability of the nanoemulsion and maintaining its functionality.<sup>34</sup>

Another important factor for emulsions and colloidal system stability evaluation is the zeta-potential factor, which accounts for the net surface charge of the particles.<sup>21</sup> From Table 1, it is observed that the zeta potential values of the essential oil coarse emulsion and nanoemulsion were -27 and -26 mV, respectively. The large charges could prevent the droplets from aggregating due to the electrostatic repulsion among them. According to Mahbubul *et al.*<sup>35</sup> droplets with an electrical charge

near to |30| mV and above are considered to be stable within the nanoemulsion system, while flocculation might occur below |15| mV. Therefore, the coarse emulsion and nanoemulsion formed in the present study could be considered stable by electrostatic mechanisms.

The optical properties of emulsions play a crucial role in their suitability for food-related applications. It was observed that the whiteness index of the *P. minor* Huds. essential oil emulsion decreased by 10.57% following the high-pressure homogeniser treatment (Table 1). According to Choi and McClements,<sup>36</sup> optical properties including colour and translucency of emulsions are mainly influenced by the oil droplet size. Small oil droplets scatter light weakly as compared to larger oil droplets. This leads to a decrease in the lightness, opacity, and whiteness index of emulsions. A nanoemulsion is generally described as a transparent system due to the reduced light scattering from the nanoscale droplet size.<sup>37</sup> Although coarse-emulsified essential oil in this present study reduced in average droplet size and distribution after homogenization, the essential oil emulsion could not produce a transparent emulsion. This could be attributed to the *P. minor* Huds. essential oil unable to solubilize in the aqueous phase. Similar to the findings of this study, Salvia-Trujillo *et al.*<sup>31</sup> also obtained a translucent nanoemulsion from various essential oils (lemongrass, clove, thyme, mint, rosewood, and sage) by using high-pressure valve homogenization (150 MPa and 3 cycles).

### Antibacterial activity of essential oil emulsions

In Fig. 2, both coarse-emulsified and nanoemulsified *P. minor* Huds. essential oil demonstrated antibacterial activity against *Escherichia coli* and *Bacillus subtilis*. The nanoemulsified



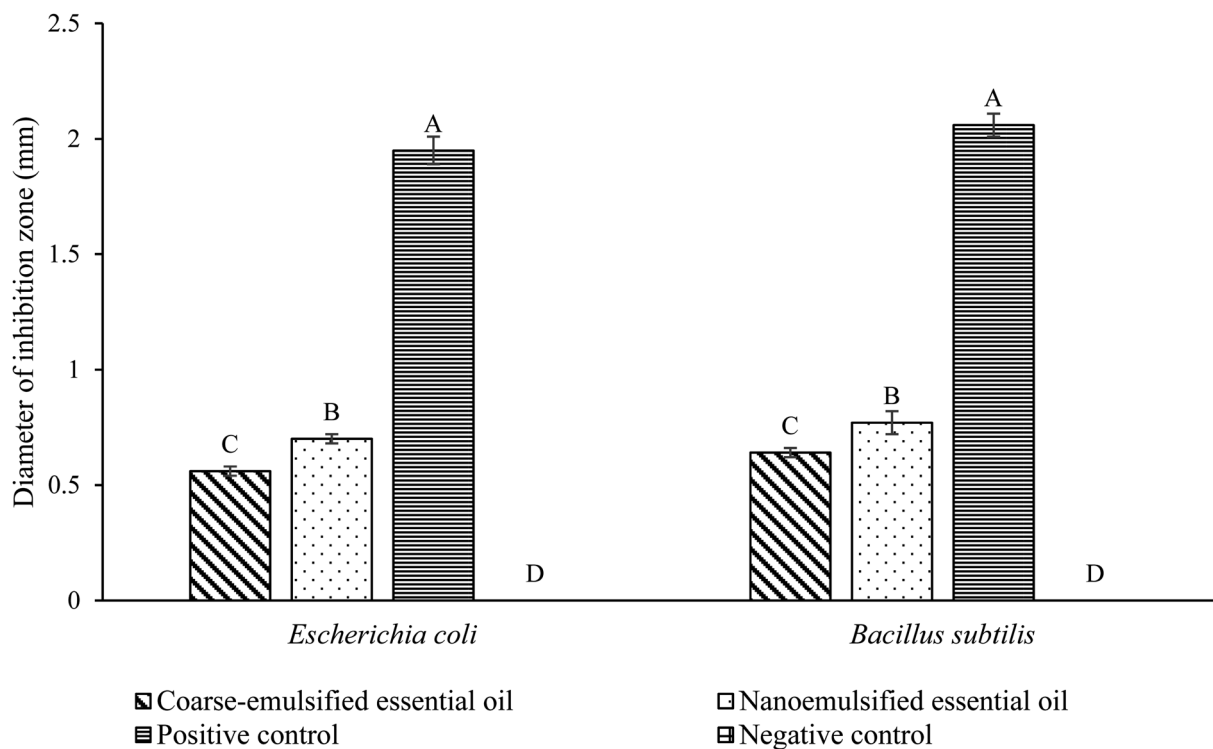


Fig. 2 Diameter of the inhibition zone (mm) of the *Persicaria minor* Huds. essential oil coarse emulsion and nanoemulsion. Tetracycline solution was used as positive control. Distilled water was used as negative control. <sup>ABCD</sup> indicates significant difference within the same bacteria ( $p < 0.05$ ) via one way ANOVA and Tukey's post-hoc test.

essential oil had an inhibition zone of 0.70 mm for *E. coli* and 0.77 mm for *B. subtilis*, while coarse-emulsified essential oil had an inhibition zone of 0.56 mm for *B. subtilis* and 0.64 mm for *E. coli*. This is attributed to the mechanism of action of essential oils against the bacteria strains. The interaction of bioactive compounds with the proteins in the cytoplasmatic membrane of the bacteria leads to leakage of ions and other cellular content, thus resulted in cell breakdown.<sup>38</sup>

*P. minor* Huds. essential oils are known to contain  $\beta$ -caryophyllene, a terpene compound that has a strong antibacterial effect with the ability to inactivate a broad spectrum of micro-organisms.<sup>39</sup> In addition, the presence of decanal and dodecanal in *P. minor* Huds. essential oils could also enhance their antibacterial activity. Although their effects may not be as significant as those of  $\beta$ -caryophyllene, these aliphatic compounds are also potent antibacterial and antifungal agents.<sup>40,41</sup> Therefore, the overall antibacterial activity of an essential oil is a combination of the composition of each volatile compound.<sup>31</sup>

Among the two types of *P. minor* Huds. essential oil emulsions, the nanoemulsion exhibited stronger antibacterial activity as compared to the coarse emulsion (Fig. 2). Similar findings were also reported for nanoemulsions containing flavour oils, such as peppermint oil,<sup>42</sup> limonene,<sup>43</sup> or eugenol and cinnamaldehyde,<sup>6</sup> where an enhancement in the antibacterial activity was observed.

A nanoemulsion-based system can increase the surface area of essential oils and facilitate their passive transport across the

outer cell membrane, leading to improved interaction with the microbial cytoplasmic membranes.<sup>44</sup> The small nanoemulsion droplets with hydrophilic surfaces can pass through the cell membrane through the abundant porin proteins that serve as hydrophilic transmembrane channels for Gram-negative bacteria.<sup>45</sup> For Gram-positive bacteria, the small nanoemulsion droplets allow the essential oils to be on the cell membrane surface, enhancing accessibility to microbial cells and enabling the disruption of the cell membrane by altering the phospholipid bilayer integrity or interfering with active transport proteins embedded in the phospholipid bilayer.<sup>46</sup> Hence, the use of the *P. minor* Huds. essential oil nanoemulsion is more suitable than the use of the coarse emulsion as the active ingredient for the potential antibacterial composite film packaging.

#### Colour of composite films with essential oil emulsions

The colour properties of the edible films are an important factor to be evaluated as they affect the appearance of the food products. The effects of nanoemulsified *P. minor* Huds. essential oil concentrations on the colour properties of the composite films are demonstrated in Table 2. As the concentration of the nanoemulsified *P. minor* Huds. essential oil increased from 0% to 12%, the film's greenness increased by 54.2%, while the yellowness increased by 32.74%. The findings indicate that a high concentration of nanoemulsified *P. minor* Huds. essential oil contributes to a yellower and greener



**Table 2** Colour difference of the carboxymethyl cellulose (CMC)–chitosan (CS) composite film with different concentrations of *Persicaria minor* Huds. essential oil nanoemulsion<sup>a</sup>

Concentration of <i>P. minor</i> Huds. essential oil nanoemulsion (% v/v)	<i>L</i> *	<i>a</i> *	<i>b</i> *	$\Delta E$
0	68.84 ± 0.03 <sup>C</sup>	−1.44 ± 0.01 <sup>A</sup>	4.98 ± 0.01 <sup>D</sup>	—
4	70.68 ± 0.05 <sup>A</sup>	−1.85 ± 0.01 <sup>B</sup>	6.75 ± 0.02 <sup>C</sup>	2.82 ± 0.05 <sup>C</sup>
8	69.63 ± 0.01 <sup>B</sup>	−2.12 ± 0.01 <sup>C</sup>	8.17 ± 0.02 <sup>B</sup>	4.58 ± 0.01 <sup>B</sup>
12	68.61 ± 0.03 <sup>D</sup>	−2.22 ± 0.01 <sup>D</sup>	8.96 ± 0.01 <sup>A</sup>	5.86 ± 0.03 <sup>A</sup>

<sup>a</sup> The results are expressed as mean ± standard deviation (*n* = 3). <sup>ABC</sup> means that in the same column there is significant difference (*p* < 0.05) via one way ANOVA and Tukey's *post-hoc* test. The total colour difference of the composite films with different concentrations of *P. minor* Huds. essential oil nanoemulsion was calculated against composite films without the *P. minor* Huds. essential oil nanoemulsion.

composite film. These findings are consistent with Lee *et al.*,<sup>25</sup> Liu *et al.*,<sup>47</sup> and Norcino *et al.*,<sup>48</sup> where the changes in lightness and greenness may be attributed to the absorption of light by nanoemulsified *P. minor* Huds. essential oil molecules, affecting the colour perception. The changes in yellow can be attributed to the natural yellow colour of the *P. minor* Huds. essential oil. Additionally, it is also likely due to the non-enzymatic browning reactions by the film components after the drying process.

The total colour difference ( $\Delta E$ ) of the composite film with nanoemulsified *P. minor* Huds. essential oil increased with the concentration of the essential oil. According to Ait Ouahioune *et al.*,<sup>49</sup>  $\Delta E$  between 2 and 10 indicates that the two colours can be distinguished by the human eye on first sight,  $\Delta E$  between 11 and 49 shows that the colour is more likely similar than dissimilar, and  $\Delta E$  between 50 and 100 is perceived as different colours. Based on the results in Table 2, the addition of 4–12% (v/v) of nanoemulsified *P. minor* Huds. essential oil had  $\Delta E$  of less than 6. This indicates that the colour differences are indistinguishable at first sight as compared to the composite film without the nanoemulsified *P. minor* Huds. essential oil. Nevertheless, the colour differences are still considered to be similar to each other ( $\Delta E$  < 10).

### Opacity of composite films with essential oil emulsions

Opacity is a crucial parameter in determining the transparency of a film, where a high opacity value indicates low transparency in film.<sup>50</sup> Fig. 3 displays the visual appearance of the composite film with different concentrations of nanoemulsified *P. minor* Huds. essential oil, while the opacity is demonstrated in Table 3. The opacity of the composite films increased by 20.38% as the concentrations of nanoemulsified *P. minor* Huds. essential oil increased from 0 to 812%. This is likely due to the natural colour of *P. minor* Huds. essential oil and the presence of nanoemulsion droplets in the film matrix blocking light passage and increasing light scattering.<sup>28</sup> Similar findings were also presented by studies with CMC films containing *Satureja hortensis* essential oil<sup>51</sup> and potato starch films containing clove essential oil.<sup>52</sup> The intensity of light-scattering phenomena mainly depends on the concentration and the extent of dispersion of the oil droplets in the film matrix. The higher droplet concentration would result in greater light-scattering intensity, and consequently increased opacity values.<sup>53</sup>

In contrast, the opacity values for the CMC-CS based composite films in the present study were found to be higher than low-density polyethylene (LDPE), a commercial plastic with an opacity value of 4.26 ( $A_{600}/\text{mm}$ ).<sup>50</sup> In many applications, transparent films are often preferred as they could enhance the packaged product's appearance and influence consumer purchase intention. However, CMC-CS based composite films with nanoemulsified *P. minor* Huds. essential oil have the potential to be used as edible film packaging with light barrier properties. This packaging may protect the colour, flavour, and nutrients of light-sensitive food products against photo-oxidation.<sup>54</sup>

### Thickness of composite films with essential oil emulsions

In Table 3, the thickness of CMC-CS based composite films with different concentrations of emulsified *P. minor* Huds. essential oil ranged from 0.10 to 0.14 mm. As per industry standards, the desired thickness for films should be less than 0.25 mm.<sup>55</sup> All the composite films with nanoemulsified *P. minor* Huds. essential oil in this study achieved the desired thickness. The thickness of the film is highly dependent on the film composition and the interaction between the constituent components of edible film.<sup>11</sup> Based on Table 3, the addition of 4–12% (v/v) nanoemulsified *P. minor* Huds. essential oil into the composite films resulted in a 20–50% increase in thickness. This observation depicts that the presence of the essential oil nanoemulsion may have weakened the hydrogen bonds and van der Waals interactions in the CMC-CS chains, thus hindering the formation of a compact film network.<sup>6</sup> Additionally, the chemical composition of *P. minor* Huds. essential oil may also induce a protruded structure during film formation, which could interact with CMC or CS to form particulates or agglomerates.<sup>56</sup> Different chemical components in *P. minor* Huds. essential oil such as decanal, dodecanal,  $\alpha$ -curcumene,  $\alpha$ -humulene, or  $\beta$ -caryophyllene may interact with the biopolymers to varying degrees, thereby resulting in varying film thickness. Chu *et al.*<sup>57</sup> had also suggested that the addition of hydrophobic additives such as Tween 80 to the film-forming solution during homogenization could increase film thickness by forming micro-droplets that disrupt the biopolymer film microstructure. Similar findings were reported by Valizadeh *et al.*,<sup>7</sup> where the CMC-CS based film thickness increased with the addition of cinnamon essential oils, glutaraldehyde, and oleic acid.



(A)



(B)



(C)



(D)



Fig. 3 Visual appearance of carboxymethyl cellulose–chitosan composite films incorporating (A) 0%, (B) 4%, (C) 8%, and (D) 12% (v/v) of *Pericaria minor* Huds. essential oil nanoemulsion.

#### Water solubility and moisture content of composite films with essential oil emulsions

Water solubility of edible films is an important characteristic as it demonstrates the films' ability to resist moisture, which is desirable for preserving intermediate to high-moisture foods.<sup>58</sup> All the composite films in this study were able to maintain their structural integrity after 30 min of agitation in water. The addition of emulsified *P. minor* Huds. essential oil into composite film had no significant effect on water solubility (Table 3). This finding is supported by Wai *et al.*<sup>54</sup> where the solubility of the composite film is affected by the polymer

matrix, however it is not affected by the addition of the active ingredient.

The water solubility of the composite film with nanoemulsified essential oil in this study ranged from 65.5 to 69.8%. This is comparable to the findings by Valizadeh *et al.*<sup>7</sup> where 57.7–90.2% water solubility was reported for CMC–CS based films with different additives. This shows that the CMC–CS based composite film with nanoemulsified *P. minor* Huds. essential oil demonstrates good water resistance.

Aside from water solubility, the moisture content of edible films is also a crucial parameter as it plays an important role in



**Table 3** Opacity, thickness, water solubility, and moisture content of the carboxymethyl cellulose (CMC)–chitosan (CS) composite film with different concentrations of *Persicaria minor* Huds. essential oil nanoemulsion<sup>a</sup>

Concentration of <i>P. minor</i> Huds. essential oil nanoemulsion (% v/v)	Opacity ( $A_{600}/\text{mm}$ )	Thickness (mm)	Water solubility (%)	Moisture content (%)
0	9.57 ± 0.43 <sup>D</sup>	0.10 ± 0.00 <sup>D</sup>	69.75 ± 0.88 <sup>A</sup>	23.18 ± 0.76 <sup>A</sup>
4	10.36 ± 0.87 <sup>C</sup>	0.12 ± 0.01 <sup>C</sup>	67.44 ± 3.63 <sup>A</sup>	22.47 ± 0.34 <sup>A</sup>
8	10.88 ± 0.65 <sup>B</sup>	0.13 ± 0.00 <sup>B</sup>	66.44 ± 1.59 <sup>A</sup>	21.55 ± 0.47 <sup>B</sup>
12	11.52 ± 0.69 <sup>A</sup>	0.15 ± 0.01 <sup>A</sup>	65.50 ± 2.41 <sup>A</sup>	19.21 ± 1.10 <sup>B</sup>

<sup>a</sup> The results are expressed as mean ± standard deviation ( $n = 3$ ). <sup>ABCD</sup> means that in the same column there is significant difference ( $p < 0.05$ ) via one way ANOVA and Tukey's *post-hoc* test.

the film's stability during storage. Based on Table 3, there is no significant difference in moisture content for the CMC–CS based composite film with 0–8% (v/v) nanoemulsified *P. minor* Huds. essential oil. Similarly, Alexandre *et al.*<sup>26</sup> also reported that the addition of a nanoemulsion loaded with a range of active compounds into gelatin–chitosan films did not affect the moisture content of the films. On the other hand, the addition of 12% (v/v) of nanoemulsified *P. minor* Huds. essential oil in the composite film showed the lowest moisture content in this study (Table 3). It is hypothesized that the hydrophobic nature of the essential oil incorporated at a sufficient level could lead to a reduction in water absorption during the film formation process.<sup>59,60</sup> Besides that, it was also anticipated that the cross-linking between the essential oil and CMC–CS would lead to lower moisture uptake.<sup>7</sup>

The combination of CMC and CS is a bio-matrix with unique properties. The strong electrostatic interactions and covalent bonds between CMC–CS biopolymers could reduce the availability of free functional groups to form hydrogen bonds with water molecules.<sup>7</sup> The moisture content of the CMC–CS based composite film with or without nanoemulsified *P. minor* Huds. essential oil in this study ranged from 19.21 to 23.18%. According to Khezrian *et al.*,<sup>11</sup> low moisture content in edible film is desirable as primary packaging. This is to ensure the edible film does not contribute moisture to the food product, which could lead to product damage and a decrease in shelf-life. Biodegradable edible films with high water content are often susceptible to microbial growth due to the presence of nutritional components.<sup>61</sup> The recommended range for moisture content of bio-based edible films is approximately 16–24%. Hence, the moisture content of the composite film with nanoemulsified *P. minor* Huds. essential oil is considered acceptable.

#### Scanning electron microscopy (SEM) of composite films with essential oil emulsions

The structural and morphological properties of the composite film could reflect the interactions among the components in the film matrix.<sup>62</sup> SEM micrographs of the surface of CMC–CS based films incorporating nanoemulsified *P. minor* Huds. essential oil are presented in Fig. 4. The surface structure of the composite film with 0% emulsified essential oil was found to be

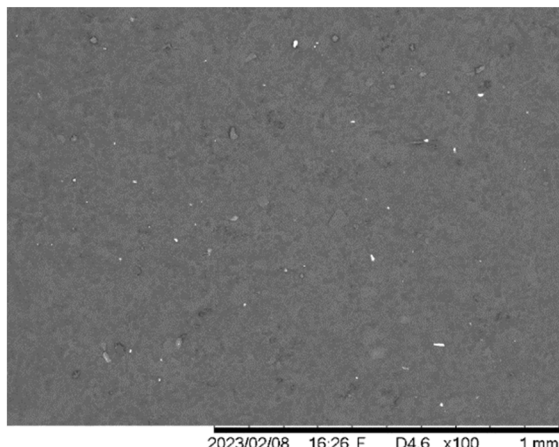
homogeneous with slight roughness, some small aggregates, and tiny pores (Fig. 4A). This indicates that there are air microbubbles that were not removed from the solution by vacuum treatment. Noshirvani *et al.*<sup>6</sup> also suggested that the lack of uniformity in the CMC–CS based films could be due to the addition of oleic acid. The presence of oleic acid might cause damage to the compact structure of the polysaccharide matrix. The droplets of oleic acid are not uniformly distributed which might introduce aggregation into the continuous polymer matrix. These findings are consistent with Perdones *et al.*<sup>63</sup> on chitosan–oleic acid films, where the presence of two distinct phases, flocculation, and partial coalescence of globules were observed.

On the other hand, the addition of 4% and 8% (v/v) nanoemulsified *P. minor* Huds. essential oil in CMC–CS based films showed more irregularities on the surface structure of the films (Fig. 4B and C). The increase in the concentrations of nanoemulsified *P. minor* Huds. essential oil resulted in varying degrees of roughness and non-homogeneity, with irregular surfaces and pores. The surface coarseness arising from the incorporation of the nanoemulsion could be attributed to the migration of essential oil nanodroplets towards the film surface. This phenomenon could be caused by the evaporation process of the volatile lipid phase, such as essential oils and Tween which have lower density than the aqueous components.<sup>64</sup> This would lead to wavy and irregular film structure formed during the drying of films.<sup>25,65</sup> Besides that, the differences in the arrangement of polysaccharide molecules during film formation may also contribute to the irregularity of the film's surface. The increase in oil content may weaken the polymer chain aggregation forces and lead to the protrusion of the film structure.<sup>66</sup>

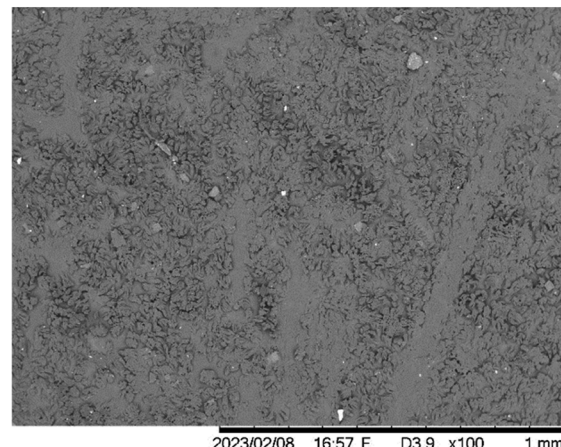
In contrast to the findings of 4% and 8% (v/v) of nanoemulsified *P. minor* Huds. essential oil, the composite film containing 12% (v/v) of nanoemulsified *P. minor* Huds. essential oil exhibits the lowest number of pores (Fig. 4D). It is hypothesized that the emulsifying properties of Tween 80 may have contributed to the stabilization of the essential oil droplets at 12% (v/v) in the composite film.<sup>62</sup> Overall, the composite film of CMC–CS incorporating 12% nanoemulsified *P. minor* Huds. essential oil displayed good compatibility with the formation of an ordered network structure.



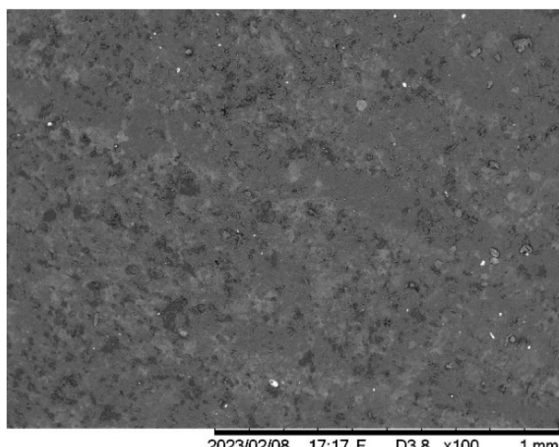
(A)



(B)



(C)



(D)

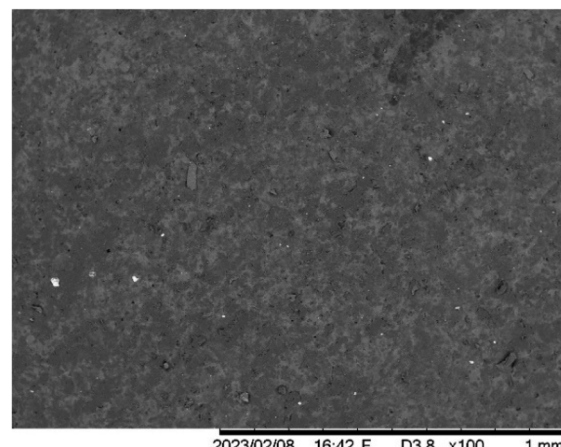


Fig. 4 Scanning electron microscopy of the surface of carboxymethyl cellulose-chitosan composite films incorporating (A) 0%, (B) 4%, (C) 8%, and (D) 12% (v/v) of *Persicaria minor* Huds. essential oil nanoemulsion.

#### Tensile strength, elongation at break and Young's modulus of composite films with essential oil emulsions

The mechanical properties such as tensile strength, elongation at break, and Young's modulus of edible films are crucial parameters as they measure the resistance to external tension forces, stretching capacity and rigidity of the film. These aspects would reflect the performance of the film packaging materials during operation and handling. The mechanical properties of CMC-CS based films incorporating different concentrations of nanoemulsified *P. minor* Huds. essential oil are given in Table 4. There was no significant difference found in tensile strength and elongation at break after the addition of nanoemulsified *P. minor* Huds. essential oil in CMC-CS based composite films ( $p > 0.05$ ). A similar finding was also reported by Azizah *et al.*<sup>67</sup> where the addition of lemongrass essential oil to the composite film did not affect the tensile strength of the film. Moreover, the elongation at break of edible film with different concentration

of emulsified oil droplets also had similar elongation at break properties.<sup>68</sup> The tensile strength and elongation at break of CMC-CS based composite films with or without nanoemulsified *P. minor* Huds. essential oil in this study ranged from 5.32 to 5.83 mPa and 43.37 to 51.20%, respectively. Both tensile strength and elongation at break values of the films are considered acceptable as they conform to the Japanese Industry Standard with a minimum of 3.92 mPa for tensile strength and good elongation at break within the range of 10–50%.<sup>54</sup>

There was also no significant difference found between the different concentrations of nanoemulsified *P. minor* Huds. essential oil in the CMC-CS based film. However, Young's modulus of the CMC-CS based composite film decreased by 33.33–42.86% after the addition of 4–12% (v/v) of essential oil nanoemulsion. The lower Young's modulus found in the CMC-CS based film with nanoemulsified *P. minor* Huds. essential oil indicates that there is an increase in flexibility and decrease in



**Table 4** Tensile strength, elongation at break, and Young's modulus of the carboxymethyl cellulose (CMC)–chitosan (CS) composite film with different concentrations of *Persicaria minor* Huds. essential oil nanoemulsion<sup>a</sup>

Concentration of <i>P. minor</i> Huds. essential oil nanoemulsion (% v/v)	Tensile strength (mPa)	Elongation at break (%)	Young's modulus (mPa)
0	5.32 ± 0.24 <sup>A</sup>	43.37 ± 2.86 <sup>A</sup>	0.21 ± 0.00 <sup>A</sup>
4	5.35 ± 0.37 <sup>A</sup>	45.90 ± 2.86 <sup>A</sup>	0.14 ± 0.00 <sup>B</sup>
8	5.59 ± 0.27 <sup>A</sup>	49.10 ± 5.94 <sup>A</sup>	0.12 ± 0.01 <sup>B</sup>
12	5.83 ± 0.30 <sup>A</sup>	51.20 ± 6.97 <sup>A</sup>	0.12 ± 0.02 <sup>B</sup>

<sup>a</sup> The results are expressed as mean ± standard deviation ( $n = 3$ ). <sup>ABCD</sup> means that in the same column there is significant difference ( $p < 0.05$ ) via one way ANOVA and Tukey's *post-hoc* test.

rigidity and resistance of the film. This finding could be attributed to the plasticising effect of the essential oil nanoemulsion droplets. The incorporation of lipids into polymer-based film-forming formulations leads to heterogeneity of biopolymer networks and reduced intermolecular interactions between polymeric chains. Moreover, the discontinuities created by the oil droplets of the nanoemulsion may have weakened the hydrogen bonds of the matrix molecules, hence destroying the internal network and cohesiveness of the matrix, allowing it to relocate the matrix chain during stretching.<sup>69</sup>

#### Antioxidant and antibacterial activity of composite films with essential oil emulsions

Lipid oxidation and protein oxidation are two of the major factors that lead to food quality deterioration during storage.<sup>70</sup> The incorporation of natural antioxidants into active packaging materials is a promising approach to extend the shelf-life of the food products. The FRAP Trolox equivalent (mg TE g<sup>-1</sup>) of film incorporating different concentrations of nanoemulsified *P. minor* Huds. essential oil is shown in Table 5. The CMC-CS based film without the essential oil demonstrated no antioxidant activity. In contrast, the FRAP antioxidant scavenging activity of composite films was enhanced ( $p < 0.05$ ) with the presence of nanoemulsified *P. minor* Huds. essential oil. The antioxidant activity of the composite film increases with the concentration of nanoemulsified *P. minor* Huds. essential oil, becoming twice as high with 12% (v/v) of nanoemulsified *P. minor* Huds. essential oil compared to that with 4% (v/v). A similar trend was reported by Ruiz-Navajas *et al.*,<sup>71</sup> where the

antioxidant activity of a chitosan film increased from 2.79 to 10.09 mg TE g<sup>-1</sup> with the incorporation of 0.5%, 1%, and 2% of *Thymus piperella* essential oil.

The antioxidant activity of *P. minor* Huds. essential oil could be related to the presence of phenolic compounds such as terpenoids. The antioxidant function of the phenolic compounds in *P. minor* Huds. essential oil could be exerted by various possible mechanisms such as free-radical scavenging activity, transition-metal-chelating activity, hydrogen donors, and singlet-oxygen-quenching capacity.<sup>71</sup> Abdullah *et al.*<sup>13</sup> showed that a *P. minor* extract demonstrated antioxidant activity with IC<sub>50</sub> values of less than 20 µg mL<sup>-1</sup> in a DPPH-scavenging assay. Additionally, the reduction of particle size from the nanoemulsifying process may lead to an increase in the specific surface area to volume ratio, thereby enhancing the scavenging effect of free radicals.<sup>20</sup>

The antibacterial activity of CMC-CS based films with different concentrations of nanoemulsified *P. minor* Huds. essential oil is presented in Fig. 5. There was no inhibitory effect against both *E. coli* and *B. subtilis* for CMC-CS based films without the addition of nanoemulsified *P. minor* Huds. essential oil, while tetracycline displayed 24.91 mm and 25.60 mm of inhibition zone against *E. coli* and *B. subtilis*, respectively. As the concentration of nanoemulsified *P. minor* Huds. essential oil in the CMC-CS based film increases from 4 to 12% (v/v), the inhibition zone increases from 4.41 to 7.19 mm against *E. coli* and 4.93 to 7.85 mm against *B. subtilis*. A similar finding was observed by Hasheminya *et al.*,<sup>72</sup> whereby the inhibition against *Listeria monocytogenes* increases with the concentration of *Salvia mirzayanii* essential oil nanoemulsion from 1 to 2%. This shows that the antibacterial activity of the edible film is highly dependent on the essential oil concentration.

Approximately 90–95% of the cell wall of Gram-positive bacteria consists of peptidoglycans, whereas the cell wall of Gram-negative bacteria is more complex, with a thinner peptidoglycan layer and an outer membrane made of a double layer of phospholipids.<sup>73</sup> Hydrophobic molecules can easily penetrate through the thick peptidoglycan layer of Gram-positive bacteria. On the other hand, the presence of an outer hydrophilic membrane embedded with lipopolysaccharide molecules on Gram-negative bacteria serves as a protective barrier towards macromolecules and hydrophobic compounds, limiting the access to the cell membrane.<sup>44</sup> This often leads to lower inhibitory activity against Gram-negative bacteria. Nevertheless, both

**Table 5** Trolox equivalent of the carboxymethyl cellulose (CMC)–chitosan (CS) composite film with different concentrations of *Persicaria minor* Huds. essential oil nanoemulsion<sup>a</sup>

Concentration of <i>P. minor</i> Huds. essential oil nanoemulsion (% v/v)	Trolox equivalent (mg TE g <sup>-1</sup> )
0	0.00 ± 0.00 <sup>C</sup>
4	2.06 ± 0.73 <sup>B</sup>
8	2.64 ± 0.59 <sup>B</sup>
12	4.25 ± 0.86 <sup>A</sup>

<sup>a</sup> The results are expressed as mean ± standard deviation ( $n = 3$ ). <sup>ABCD</sup> means that in the same column there is significant difference ( $p < 0.05$ ) via one way ANOVA and Tukey's *post-hoc* test.



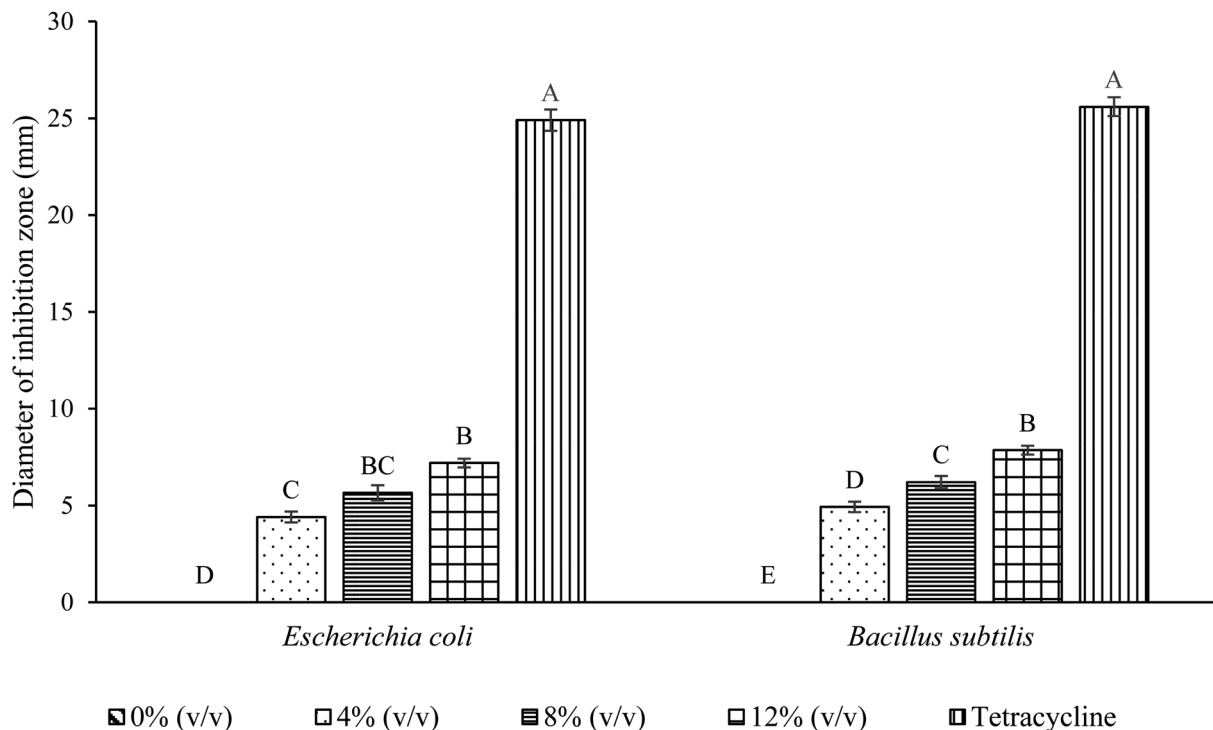


Fig. 5 Diameter of the inhibition zone (mm) of the carboxymethyl cellulose–chitosan composite films incorporating different concentration of *Persicaria minor* Huds. essential oil nanoemulsion. A tetracycline disc was used as positive control. <sup>ABCDE</sup> indicates significant difference within the same bacteria ( $p < 0.05$ ) via one way ANOVA and Tukey's post-hoc test.

Gram-positive and Gram-negative bacteria were able to be inhibited by the composite film with nanoemulsified *P. minor* Huds. essential oil in this study.

## Conclusions

The *P. minor* Huds. essential oil nanoemulsion demonstrated a smaller droplet size, lower polydispersity index, and lower whiteness index than the coarse emulsion, with acceptable zeta-potential. The *P. minor* Huds. essential oil also had higher antibacterial activity against *E. coli* and *B. subtilis* through the nanoemulsifying process. As the concentration of nanoemulsified *P. minor* Huds. essential oil in the CMC-CS based composite films increases, the colour differences, opacity, and thickness of the film increases. On the other hand, there was no effect on the water solubility, tensile strength, and elongation at break after the addition of nanoemulsified essential oil in the composite film, except for Young's modulus, which was lowered. The CMC-CS based composite film with 12% (v/v) of nanoemulsified *P. minor* Huds. essential oil exhibited the most promising characteristics with the highest antibacterial and antioxidant activity, lowest moisture content, and least pores from the microstructure. This shows its potential use as bioactive packaging for food products. Future study could further optimise the surfactant to improve the zeta potential of the nanoemulsion. Furthermore, shelf-life study of food products packaged in CMC-CS based composite film with nanoemulsified *P. minor* Huds. essential oil could also be investigated.

## Conflicts of interest

The authors confirm that they have no conflicts of interest with respect to the work described in this manuscript.

## Acknowledgements

This study is supported by UCSI University under the Ministry of Higher Education Malaysia under the Fundamental Research Grant Scheme (FRGS/1/2020/STG01/UCSI/02/3).

## References

- 1 R. Chawla, S. Sivakumar and H. Kaur, Antimicrobial edible films in food packaging: current scenario and recent nanotechnological advancements-a review, *Carbohydr. Polym. Technol.*, 2021, **2**, 100–124.
- 2 P. Umaraw, et al., Edible films/coating with tailored properties for active packaging of meat, fish and derived products, *Trends Food Sci. Technol.*, 2020, **98**, 10–24.
- 3 S. A. Mohamed, M. El-Sakhawy and M. A. M. El-Sakhawy, Polysaccharides, protein and lipid-based natural edible films in food packaging: a review, *Carbohydr. Polym.*, 2020, **238**, 116–178.
- 4 Y. Shahbazi, Characterization of nanocomposite films based on chitosan and carboxymethylcellulose containing *Ziziphora clinopodioides* essential oil and *methanolic Ficus carica* extract, *J. Food Process. Preserv.*, 2018, **42**(3), 134–144.



5 A. R. Ferreira, V. D. Alves and I. M. Coelhoso, Polysaccharide-based membranes in food packaging applications, *Membranes*, 2016, **6**(2), 22.

6 N. Noshirvani, et al., Cinnamon and ginger essential oils to improve antifungal, physical and mechanical properties of chitosan-carboxymethyl cellulose films, *Food Hydrocolloids*, 2017, **70**, 36–45.

7 S. Valizadeh, et al., Development of bioactive composite films from chitosan and carboxymethyl cellulose using glutaraldehyde, cinnamon essential oil and oleic acid, *Int. J. Biol. Macromol.*, 2019, **134**, 604–612.

8 A. Gregorova, et al., Hydrothermal effect and mechanical stress properties of carboxymethylcellulose based hydrogel food packaging, *Carbohydr. Polym.*, 2015, **117**, 559–568.

9 D. Hu, H. Wang and L. Wang, Physical properties and antibacterial activity of quaternized chitosan/carboxymethyl cellulose blend films, *LWT-Food Sci. Technol.*, 2016, **65**, 398–405.

10 P. Singh, et al., Development of carboxymethyl cellulose-chitosan hybrid micro-and macroparticles for encapsulation of probiotic bacteria, *Carbohydr. Polym.*, 2017, **175**, 87–95.

11 A. Khezrian and Y. Shahbazi, Application of nanocomposite chitosan and carboxymethyl cellulose films containing natural preservative compounds in minced camel's meat, *Int. J. Biol. Macromol.*, 2018, **106**, 1146–1158.

12 H. E. Salama, M. S. A. Aziz and M. W. Sabaa, Development of antibacterial carboxymethyl cellulose/chitosan biguanidine hydrochloride edible films activated with frankincense essential oil, *Int. J. Biol. Macromol.*, 2019, **139**, 1162–1167.

13 M. Z. Abdullah, et al., Anti-proliferative, *in vitro* antioxidant, and cellular antioxidant activities of the leaf extracts from *Polygonum minus* Huds: effects of solvent polarity, *Int. J. Food Prop.*, 2017, **20**(1), 846–862.

14 P. Chanprapai, I. Kubo and W. Chavasiri, *Anti-rice Pathogenic Microbial Activity of Persicaria Sp. Extracts*, Sci & Technology Asia, 2018, 32–41.

15 L. Pavoni, et al., Green nanoemulsion interventions for biopesticide formulations, *In Nano-Biopesticides Today and Future Perspectives*, 2019, 133–160.

16 R. Severino, et al., Antimicrobial effects of modified chitosan-based coating containing nanoemulsion of essential oils, modified atmosphere packaging and gamma irradiation against *Escherichia coli* O157: H7 and *Salmonella Typhimurium* on green beans, *Food Control*, 2015, **50**, 215–222.

17 G. Davidov-Pardo and D. J. McClements, Resveratrol encapsulation: designing delivery systems to overcome solubility, stability and bioavailability issues, *Trends Food Sci. Technol.*, 2014, **38**(2), 88–103.

18 C. C. Koga, S. Y. Lee and Y. Lee, Consumer acceptance of bars and gummies with unencapsulated and encapsulated resveratrol, *J. Food Sci.*, 2016, **81**(5), 1222–1229.

19 G. Singh, et al., Chemistry, antioxidant and antimicrobial investigations on essential oil and 680 oleoresins of *Zingiber officinale*, *Food Chem. Toxicol.*, 2008, **46**, 3295–3302.

20 S. Noori, F. Zeynali and H. Almasi, Antimicrobial and antioxidant efficiency of nanoemulsion-based edible coating containing ginger (*Zingiber officinale*) essential oil and its effect on safety and quality attributes of chicken breast fillets, *Food Control*, 2018, **84**, 312–320.

21 A. Acevedo-Fani, et al., Edible films from essential-oil-loaded nanoemulsions: physicochemical characterization and antimicrobial properties, *Food Hydrocolloids*, 2015, **47**, 168–177.

22 H. H. Gahrue, et al., Characterization of basil seed gum-based edible films incorporated with *Zataria multiflora* essential oil nanoemulsion, *Carbohydr. Polym.*, 2017, **166**, 93–103.

23 G. Zuo, et al., Physical and structural characterization of edible bilayer films made with zein and corn-wheat starch, *J. Saudi Soc. Agric. Sci.*, 2019, **18**(3), 324–331.

24 Y. L. Kuan, et al., Physicochemical properties of sodium alginate edible film incorporated with mulberry (*Morus australis*) leaf extract, *Pertanika J. Trop. Agric. Sci.*, 2020, **43**(3), 359–376.

25 J. Y. Lee, et al., Antibacterial and antioxidant properties of hydroxypropyl methylcellulose-based active composite films incorporating oregano essential oil nanoemulsions, *LWT-Food Sci. Technol.*, 2019, **106**, 164–171.

26 E. M. C. Alexandre, et al., Gelatin-based films reinforced with montmorillonite and activated with nanoemulsion of ginger essential oil for food packaging applications, *Food Packag. Shelf Life*, 2016, **10**, 87–96.

27 E. Rincón, et al., Effect of bay leaves essential oil concentration on the properties of biodegradable carboxymethyl cellulose-based edible films, *Materials*, 2019, **12**(15), 2356.

28 S. Jancikova, et al., Chemical and physical characteristics of edible films, based on  $\kappa$ -and  $\iota$ -carrageenans with the addition of lapacho tea extract, *Foods*, 2020, **9**(3), 357.

29 S. K. Hasan, G. Ferrentino and M. Scampicchio, Nanoemulsion as advanced edible coatings to preserve the quality of fresh-cut fruits and vegetables: a review, *Int. J. Food Sci. Technol.*, 2020, **55**(1), 1–10.

30 N. Amiri, et al., Nanoencapsulation (*in vitro* and *in vivo*) as an efficient technology to boost the potential of garlic essential oil as alternatives for antibiotics in broiler nutrition, *Animal*, 2021, **15**(10), 100–122.

31 L. Salvia-Trujillo, et al., Effect of processing parameters on physicochemical characteristics of microfluidized lemongrass essential oil-alginate nanoemulsions, *Food Hydrocolloids*, 2013, **30**(7), 401–407.

32 Y. Xiong, et al., Effect of oregano essential oil and resveratrol nanoemulsion loaded pectin edible coating on the preservation of pork loin in modified atmosphere packaging, *Food Control*, 2020, **114**, 107226.

33 S. M. Hashemnejad, et al., Thermoresponsive nanoemulsion-based gel synthesized through a low-energy process, *Nat. Commun.*, 2019, **10**(1), 1–10.

34 M. L. Zambrano-Zaragoza, et al., Nanosystems in edible coatings: a novel strategy for food preservation, *Int. J. Mol. Sci.*, 2018, **19**(3), 705.



35 I. M. Mahbubul, et al., Effect of ultrasonication duration on colloidal structure and viscosity of alumina-water nanofluid, *Ind. Eng. Chem. Res.*, 2014, **53**(16), 6677–6684.

36 D. J. McClements and S. J. Choi, Nanoemulsions as delivery systems for lipophilic nutraceuticals: strategies for improving their formulation, stability, functionality and bioavailability, *Food Sci. Biotechnol.*, 2020, **29**(2), 149–168.

37 Z. Wang, et al., Preparation and characterization of micro/nano-emulsions containing functional food components, *Jpn. J. Food Eng.*, 2015, **16**(4), 263–276.

38 N. Chimnoi, et al., Characterization of essential oil from *Ocimum gratissimum* leaves: Antibacterial and mode of action against selected gastroenteritis pathogens, *Microb. Pathog.*, 2018, **118**, 290–300.

39 P. V. Christopher, et al., Review on *Polygonum minus*. Huds, a commonly used food additive in Southeast Asia, *Pharmacogn. Res.*, 2015, **7**(1), 1–6.

40 R. Ahmad, et al., Volatile profiling of aromatic traditional medicinal plant, *Polygonum minus* in different tissues and its biological activities, *Molecules*, 2014, **19**(11), 19220–19242.

41 P. V. Christopher, et al., Review on *Polygonum minus*. Huds, a commonly used food additive in Southeast Asia, *Pharmacogn. Res.*, 2015, **7**(1), 115–131.

42 Q. Liu, et al., Preparation of peppermint oil nanoemulsions: Investigation of stability, antibacterial mechanism and apoptosis effects, *Colloids Surf., B*, 2021, **201**, 111626.

43 C. Y. Hou, et al., Effect of D-Limonene Nanoemulsion Edible Film on Banana (*Musa sapientum* Linn.) Post-Harvest Preservation, *Molecules*, 2022, **27**(19), 1–18.

44 F. Donsì and G. Ferrari, Essential oil nanoemulsions as antimicrobial agents in food, *J. Biotechnol.*, 2016, **233**, 106–120.

45 F. Nazzaro, et al., Effect of essential oils on pathogenic bacteria, *Pharmaceuticals*, 2013, **6**(12), 1451–1474.

46 R. Moghimi, et al., Superior antibacterial activity of nanoemulsion of *Thymus daenensis* essential oil against *E. coli*, *Food Chem.*, 2016, **194**, 410–415.

47 X. Liu, et al., Cinnamon essential oil nanoemulsions by high-pressure homogenization: Formulation, stability, and antimicrobial activity, *LWT-Food Sci. Technol.*, 2021, **147**, 111–126.

48 L. B. Norcino, et al., Pectin films loaded with copaiba oil nanoemulsions for potential use as bio-based active packaging, *Food Hydrocolloids*, 2020, **106**, 805–862.

49 L. Ait Ouahoune, et al., *Ceratonia siliqua* L. kibbles, seeds and leaves as a source of volatile bioactive compounds for antioxidant food biopackaging applications, *Food Packag. Shelf Life*, 2022, **31**, 100764.

50 D. Hermawan, et al., Development of seaweed-based bamboo microcrystalline cellulose films intended for sustainable food packaging applications, *BioResources*, 2019, **14**(2), 3389–3410.

51 H. Zohreh, et al., Antimicrobial and physicochemical properties of plasma treated bio-coating polypropylene films containing *satureja hortensis* essential oil, *Iran. J. Chem. Chem. Eng.*, 2021, **40**(4), 1216–1228.

52 S. Zhelyazkov, Physical and barrier properties of clove essential oil loaded potato starch edible films, *Biointerface Res. Appl. Chem.*, 2022, **12**(4), 4603–4612.

53 S. F. Hosseini, et al., Bio-based composite edible films containing *Origanum vulgare* L. essential oil, *Ind. Crops Prod.*, 2015, **67**, 403–413.

54 S. N. Wai, et al., Chitosan – sodium caseinate composite edible film incorporated with probiotic *Limosilactobacillus fermentum*: Physical properties, viability, and antibacterial properties, *Foods*, 2022, **11**, 3583.

55 R. A. Santos and Y. Atma, Physical properties of edible films from Pangasius catfish bone gelatin-breadfruits strach with different formulations, *Indones. Food Sci. Technol. J.*, 2020, **3**, 42–47.

56 R. Syafiq, et al., Antimicrobial activity, physical, mechanical and barrier properties of sugar palm based nanocellulose/starch biocomposite films incorporated with cinnamon essential oil, *J. Mater. Res. Technol.*, 2021, **11**, 144–157.

57 Y. Chu, et al., Evaluations of physicochemical and biological properties of pullulan-based films incorporated with cinnamon essential oil and Tween 80, *Int. J. Biol. Macromol.*, 2019, **122**, 388–394.

58 S. Galus and J. Kadzińska, Moisture sensitivity, optical, mechanical and structural properties of whey protein-based edible films incorporated with rapeseed oil, *Food Technol. Biotechnol.*, 2016, **54**(1), 78–89.

59 M. I. Socaciu, et al., Formulation and characterization of antimicrobial edible films based on whey protein isolate and tarragon essential oil, *Polymers*, 2020, **12**(8), 1–21.

60 E. Tavassoli-Kafrani, H. Shekarchizadeh and M. Masoudpour-Behabadi, Development of edible films and coatings from alginates and carrageenans, *Carbohydr. Polym.*, 2016, **137**, 360–374.

61 M. W. Apriliyani, et al., Characteristics of moisture content, swelling, opacity and transparency with addition chitosan as edible films/coating base on casein, *Adv. J. Food Sci. Technol.*, 2020, **18**(1), 9–14.

62 Y. Zhou, et al., Effects of cinnamon essential oil on the physical, mechanical, structural and thermal properties of cassava starch-based edible films, *Int. J. Biol. Macromol.*, 2021, **184**, 574–583.

63 Á. Perdones, et al., Physical, antioxidant and antimicrobial properties of chitosan–cinnamon leaf oil films as affected by oleic acid, *Food Hydrocolloids*, 2014, **36**, 256–264.

64 S. M. Jafari, Lipid-Based Nanostructures for Food Encapsulation Purposes: Volume 2 in the Nanoencapsulation in the Food Industry series, Academic Press, vol. 2, 2019.

65 H. Lian, et al., Effect of emulsifier hydrophilic-lipophilic balance (HLB) on the release of thyme essential oil from chitosan films, *Food Hydrocolloids*, 2019, **97**, 105–213.

66 C. D. G. Tovar, et al., Synthesis, characterization, and histological evaluation of chitosan-*Ruta graveolens* essential oil films, *Molecules*, 2020, **25**(7), 1688.

67 F. Azizah, et al., Development of edible composite film from fish gelatin–pectin incorporated with lemongrass essential



oil and its application in chicken meat, *Polymers*, 2023, **15**(9), 1–18.

68 S. D. Tabatabaei, et al., Effect of emulsified oil droplets and glycerol content on the physicochemical properties of Persian gum-based edible films, *Polym. Test.*, 2022, **106**, 107427.

69 C. G. Otoni, et al., Recent advances on edible films based on fruits and vegetables—A review, *Compr. Rev. Food Sci. Food Saf.*, 2017, **16**(5), 1151–1169.

70 L. Cai and Y. Wang, Physicochemical and antioxidant properties based on fish sarcoplasmic protein/chitosan composite films containing ginger essential oil nanoemulsion, *Food Bioprocess Technol.*, 2021, **14**, 151–163.

71 Y. Ruiz-Navajas, et al., *In vitro* antibacterial and antioxidant properties of chitosan edible films incorporated with *Thymus moroderi* or *Thymus piperella* essential oils, *Food Control*, 2013, **30**(2), 386–392.

72 S. M. Hasheminya and J. Dehghannya, Development and characterization of novel edible films based on *Cordia dichotoma* gum incorporated with *Salvia mirzayanii* essential oil nanoemulsion, *Carbohydr. Polym.*, 2021, **257**, 117–121.

73 H. Majeed, et al., Influence of carrier oil type, particle size on *in vitro* lipid digestion and eugenol release in emulsion and nanoemulsions, *Food Hydrocolloids*, 2016, **52**, 415–422.

